PHYSICAL REVIEW B **73**, 195306 (2006)

Mechanism for increasing dopant incorporation in semiconductors via doped nanostructures

Igor L. Kuskovsky,[1,2,*] Y. Gu,[2,†] Y. Gong,[2] H. F. Yan,[2] J. Lau,[2,4] I. C. Noyan,[2] G. F. Neumark,[2] O. Maksimov,[3]
X. Zhou,[3] M. C. Tamargo,[3] V. Volkov,[4] Y. Zhu,[4] and L. Wang[5]
[1]*Department of Physics, Queens College of CUNY, Flushing, New York 11367, USA*
[2]*Department of Applied Physics and Applied Mathematics, Columbia University, New York, New York 10027, USA*
[3]*Department of Chemistry, City College of CUNY, New York, New York 10036, USA*
[4]*Materials Science Division, Brookhaven National Laboratory, Upton, New York 11973, USA*
[5]*Charles Evans & Associates, 810 Kifer, Sunnyvale, California 94086, USA*
(Received 22 February 2006; revised manuscript received 6 April 2006; published 8 May 2006)

A long-standing problem for ZnSe (and related alloys) has been to obtain good *p*-type doping. Recent work has given about an order-of-magnitude improvement in such doping by use of Te as a "codopant" to facilitate the introduction of an acceptor dopant (N), since it is known that *p*-ZnTe can be obtained quite readily; the Te was introduced in submonolayer quantities via planar (δ) doping during molecular beam epitaxy. Here, we examine the mechanism of this improved doping. We show that it resides in the formation of ZnTe-rich nanoislands, with the N embedded in these. This result is obtained by studies involving transmission electron microscopy, high-resolution x-ray diffraction, secondary-ion mass spectroscopy, and temperature quenching of photoluminescence. We note that these nanoislands appear quite unique, in providing doping of semiconductors, and thus are of great interest of their own.

DOI: 10.1103/PhysRevB.73.195306 PACS number(s): 78.67.Pt, 78.66.Hf, 81.07.Ta

It is well known that it has been difficult to obtain "adequate" (high) bipolar conductivity in wide-band-gap semiconductors, and that this problem resides in obtaining adequate dopant incorporation due to poor solubility and/or excessive compensation (e.g. Refs. 1–4). It is also well known that in some wide-band-gap semiconductors it is easy to incorporate *n*-type dopants, whereas in others *p*-type doping is easy; the cause for this behavior is of great physical interest, but microscopic models (e.g., Refs. 5–8 and references therein) are still limited in scope or not yet well established. In any case, we have utilized[9,10] this type of behavior to obtain about an order-of-magnitude improvement in dopant incorporation in *p*-type Zn(Be)Se, a material which is notoriously difficult to dope *p* type. Specifically, we grew the Zn(Be)Se via molecular beam epitaxy (MBE) and incorporated δ-layers containing N as acceptor dopant and Te as "codopant" (i.e., material used to facilitate introduction of the dopant); Te was used since it is known that *p*-ZnTe can be readily obtained (e.g., Ref. 11 and references therein). Two types of samples were grown, one with insertion of a single δ-layer (δ-doped samples), the other with insertion of three contiguous δ-layers (δ^3-doped samples) between nominally undoped ZnSe layers, which hereforth we shall refer to as spacers; we note that it was the latter samples that showed the most improved doping.[9,10] We further note that very small amounts of Te were used, resulting in a coverage of $\sim$0.25 monolayer (ML) (here 1 ML is half of the unit cell) as obtained from high-resolution x-ray diffraction (HRXRD) (see below).

In the present paper, we present evidence that the microscopic mechanism leading to this improved doping (in the δ^3-doped samples) resides in N being embedded in nanoislands rich in ZnTe.[12] Moreover, it also must be emphasized that these Te-N nanostructures are of a unique type (to the best of our knowledge) having the property that they provide doping in semiconductors, and thus are of very great interest on their own. The evidence for the ZnTe:N nanoislands is given by (i) transmission electron microscopy (TEM), which showed that the δ-regions do not form continuous planes; thus, there must be formation of islands, which, as shown below, are nanosized; (ii) HRXRD which showed that δ-regions are rich in ZnTe, i.e., the nanoislands are Te rich; (iii) secondary-ion mass spectroscopy (SIMS) in conjunction with electrochemical capacitance-voltage (ECV) profiling, which showed that both N and Te stay together within the δ-region and that N does not form compensating complexes, as it does in bulk ZnSe:N (see, e.g., Refs. 13–16 and references therein); (iv) the temperature quenching of photoluminescence (PL), from which we show that the resultant values of the N acceptor activation energies can be explained only by assuming that N is embedded preferentially in a ZnTe-rich environment.

Various sample configurations based on the basic sample structure shown in Fig. 1(a) were designed for a specific characterization technique (TEM, HRXRD, and SIMS) to achieve the optimal results. For HRXRD, "standard"[9] samples were grown with a Te+N deposition time of 5 s and with 10 ML ZnSe (nominally undoped) spacer regions; for TEM, a sample with a 20 s Te+N deposition time [which is longer than the standard time, in order to enhance the TEM contrast associated with the substitution of Se by Te (Ref. 17)] and 6 ML spacers (nominally undoped ZnSe) was prepared; for SIMS, a "supersample," consisting of four basic sample structures (with 48 ML spacers) obtained by changing the (Te+N) deposition time from 5 to 40 s [regions A, B, C, and D in Fig. 1(b)], separated by 300-nm-thick ZnSe buffers, was grown.

We first discuss the TEM results. Bright- dark-field imaging, high-resolution electron microscopy (HREM), and selective area electron diffraction (SAED) obtained from a

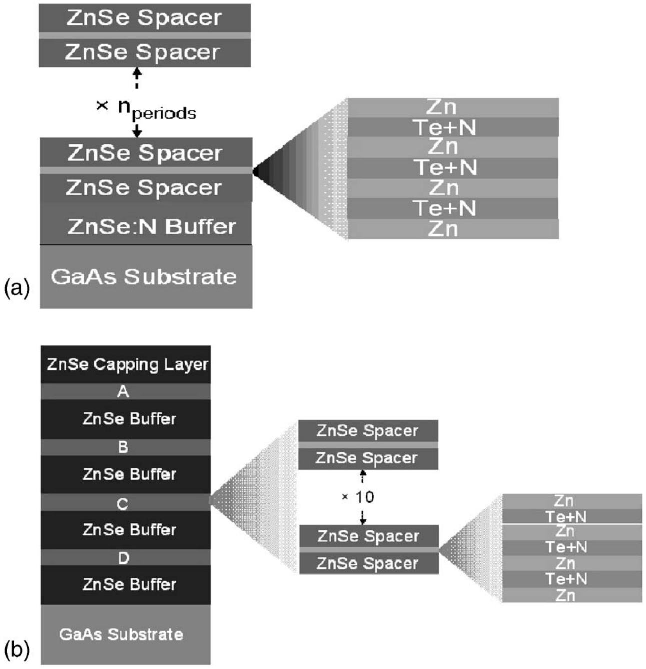

FIG. 1. Schematics of (a) a basic sample structure and (b) a supersample, which consists of four subsamples (A, B, C, and D) with 40, 20, 10, and 5 s Te+N deposition time for A, B, C, and D, respectively. Each subsample was grown with 48 ML ZnSe spacers.

cross-sectional TEM specimen are shown in Figs. 2(a), 2(b), and 2(c), respectively. The samples were viewed along the [100] direction.

The direct TEM and HREM observations [Figs. 2(a) and 2(b)] show the presence of a modulated structure with an optical period of 1.5–1.7 nm along the growth direction ([001]), whereas this is absent in the ZnSe buffer layer as well as in the substrate. This period is in excellent agreement with the thickness (nominally ~1.4–1.7 nm) of the spacer layers in this sample. Moreover, and this is highly significant, the TEM images consistently show a discontinuity of the modulated structure [Fig. 2(a)] in the basal plane; thus, this modulated structure is not a perfect superlattice (SL). Therefore one can conclude that nanoislands of an optical size below 15 nm [Figs. 2(a) and 2(b)] are formed in the (001) plane. Further confirmation of both the nanoisland formation and the modulated structure is given by the SAED results. Thus, as seen in SAED, satellite spots [Fig. 2(c) and the inset] are present along with the primary ZnSe reflections, confirming the existence of a modulated structure. These spots exhibit an elongated shape within the (001) plane, which means that no full SL is formed. In fact, if a perfect SL existed, then such satellites would form SL reflections in the diffraction pattern with "perfect dots" instead. Using the ZnSe {001} and {020} reflections as references we have determined that the period of the modulated structure is 1.6±0.1 nm, in excellent agreement with our direct observations [Figs. 2(a) and 2(b)]. Using the observed elongation, and assuming that the intensity of the satellite spots can be described by a Gaussian profile, we have estimated that the minimum statistically significant size of the features in the (001) plane is ~1.9 nm.[18] Furthermore, assigning this to be the island size, we conclude that the Te-rich nanoislands have a lateral size between ~2 and 15 nm. We note here that the upper limit for the nanoislands in our standard (5 s deposition) samples is expected to be smaller than that given by the present sample (longer Te deposition time gives larger islands[19]). We note that the TEM results are also supported by reflection high-energy electron diffraction (RHEED) oscillations, observed during the growth, which suggested that no full ZnTe monolayers are formed. An additional TEM result is that, overall, the periodic atomic structure of the δ^3-ZnSe:(Te,N) system seems largely preserved and there is no indication that misfit dislocations are formed [Fig. 2(b)].

For further information on the structural properties, we also measured HRXRD at beamline X20A of the National Synchrotron Light Source (NSLS) at Brookhaven National Laboratory (BNL). In Fig. 3 we show the (004) θ-2θ scan (solid black line) of a standard sample. The strongest peak at $2\theta \simeq 66.01°$ is from the GaAs substrate. In addition, satellite peaks associated with the periodic structure along the growth direction are observed. This confirms periodicity not only for the specially grown TEM samples, but also for standard ones. A simulation[20] of the HRXRD curve allows a direct determination of such parameters as the δ-layer and spacer thicknesses (d_δ and d_{sp}, respectively) as well as the corresponding Te concentrations. The best fit [dashed (green) line] was obtained with $d_\delta \sim 0.25$ ML and $d_{sp} \sim 10.4$ ML, which

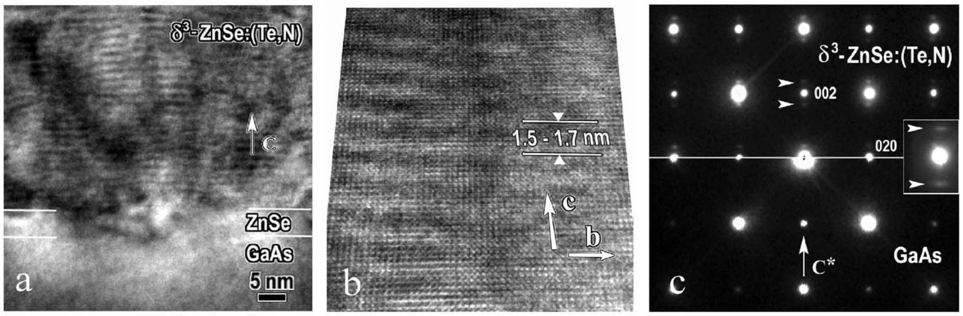

FIG. 2. Microstructure of a sample with ~5–6 ML thick spacers and 20 s Te+N deposition time. (a) TEM image taken at medium magnification along the [100] zone axis, showing modulated structure in the film; (b) a high-resolution image shown at grazing angle to enhance modulation contrast, revealing the absence of misfit dislocations; (c) composite SAED pattern corresponding to (a), revealing elongated satellite reflections (enlarged in the inset) associated with this modulation.

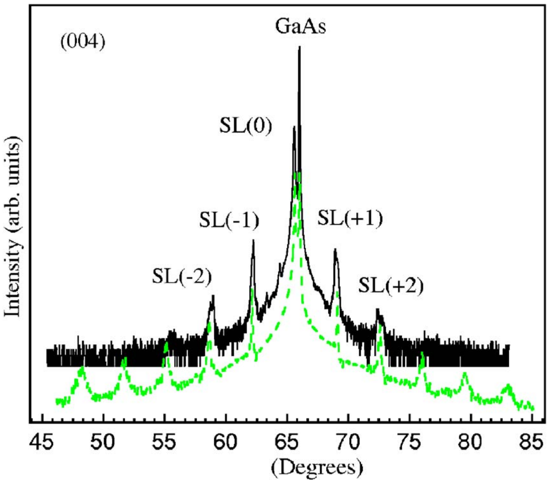

FIG. 3. (Color online) The (004) θ-2θ scan [solid (black) line] of a sample with ~10 ML thick spacers and 5 s Te+N deposition time. The dashed (green) line is the best-fit simulation, using dynamical diffraction theory.

are in excellent agreement with the nominal growth parameters; the average Te concentrations are 37% and 2.2% in the δ-layers and the spacers, respectively. Moreover, a broadening of the satellite peaks was observed; this was modeled during the simulations by a period dispersion (e.g., Ref. 21 and references therein). Furthermore, the low coverage and relatively high Te concentration within the δ^3-layers indicate that Te is not uniformly distributed within these layers, and, thus, forms ZnTe-rich nanoislands (ZnTe and ZnSe type-II quantum dots have been observed optically in similar samples grown without nitrogen[22]). The high Te concentration in the δ-layers is consistent with doping results obtained for ZnSeTe alloys, where it was shown that high acceptor concentrations are observed only for Te concentrations exceeding 15%.[11] The incorporation of minute quantities of Te into the nominally undoped spacer regions is most likely due to the Te presence in the molecular beam epitaxy chamber even after the Te shutters are closed.

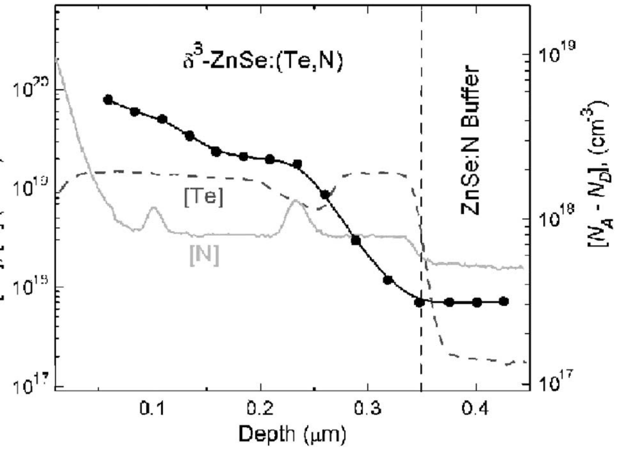

FIG. 4. SIMS and ECV profiles for a sample with ~10 ML thick spacers and 5 s Te+N deposition time. Left scale: dashed line is the total Te concentration, solid line is the total N concentration. Right scale: solid circles are net acceptor concentration. The vertical dashed line represents the border between the film (δ layers and spacers) and the ZnSe:N buffer layer.

Having established the existence of a periodic structure of these nanoislands, we next discuss results of SIMS measurements in combination with ECV depth profiling.[23] First we show SIMS (Fig. 4) on a standard sample together with the depth profile of the net acceptor concentration ($[N_A-N_D]$) (N_A and N_D are the total acceptor and donor concentrations, respectively) obtained via ECV profiling obtained previously (see Ref. 9). This gives a direct comparison between $[N_A-N_D]$ and the total nitrogen concentration. The average [N] in the film (δ-layers and spacers) is only slightly higher than that in the ZnSe:N buffer, which is probably due to an increased solubility in the presence of Te.[24] On the other hand, $[N_A-N_D]$ in the film and buffer are dramatically different: in the film, $[N_A-N_D]\approx[\mathrm{N}]$, whereas in the buffer layer $[N_A-N_D]$ is only one-tenth of [N]. Moreover, $[N_A-N_D]$ decreases only when the concentration of Te decreases drastically. This low $[N_A-N_D]$ is consistent with extensive evidence that a large portion of nitrogen in bulk ZnSe:N is incorporated on "compensating" sites (e.g., Refs. 13–19). It is of great importance that $[N_A-N_D]$ in the film with δ-regions is far higher, and we thus conclude that in the δ^3-doped ZnSe:(Te,N) nitrogen stays preferentially within the ZnTe environment, where it acts as an acceptor.

To further confirm that Te and N are located spatially preferentially within the same regions, we performed SIMS on the supersample,[25] which had thicker spacers so that one could identify the position of N and Te within the δ-layers. Indeed, the periodic, synchronous variations in the Te and the N compositions are clearly seen in Fig. 5, especially in the top portion of the supersample, where the SIMS resolution is the highest.[26] These variations occur on the scale of 10–11 nm, which is in good agreement with the nominal spacer thickness (48 ML). In other words, in our current system, even given the low Te coverage, the Te "locks" the nitrogen in place, preventing its diffusion into the ZnSe spac-

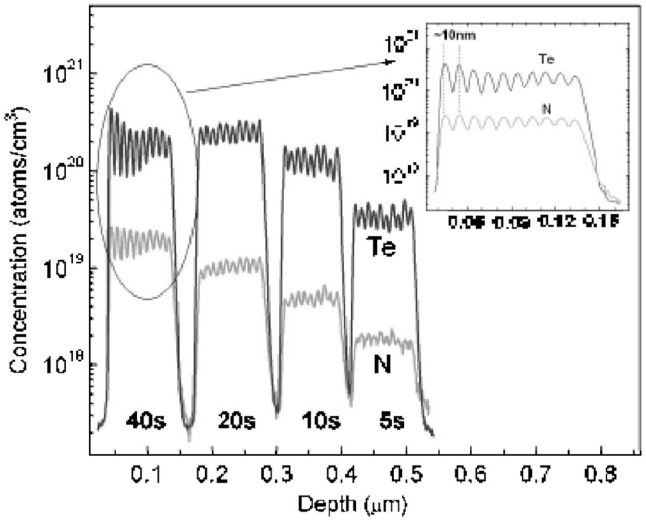

FIG. 5. SIMS profile for the supersample [schematics shown in Fig. 1(b)] showing concurrent periodic variations in Te and N concentrations on the scale of ~10 nm.

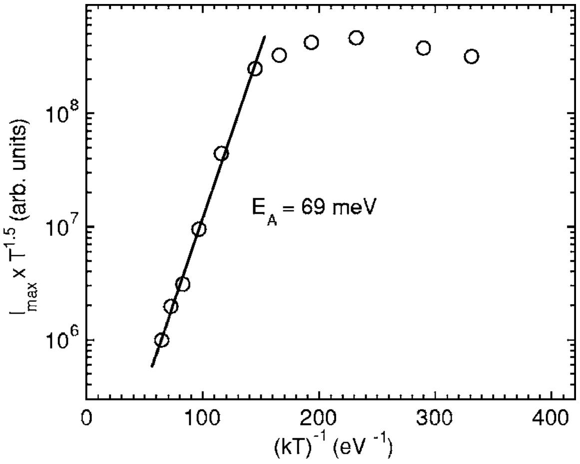

FIG. 6. PL of one typical sample (circles) at various temperatures. Solid line is from fitting.

ers, where it would behave as a donor, increasing compensation in the ZnSe:N, and causing devices failures.[13,15]

Still further, independent, evidence for nitrogen incorporation into Te-rich nanoislands is given by temperature quenching of the PL (Fig. 6). For the detailed description of PL see Ref. 27. The resultant activation energy of N in δ^3-doped samples is appreciably lower (see Table I) than that in ZnSe, being 38–87 meV,[28] vs 111 meV in ZnSe;[29] we note that the N activation energy in ZnTe has been reported as 30–65 meV,[30–32] i.e., our values are close to those in ZnTe. These results show that the N must be located in a nanoisland, which contains a relatively large fraction of Te as next-nearest neighbors (Zn atoms are the nearest neighbors). Moreover, this activation energy decreases with increasing Te concentration (Table I). This is as expected: a higher Te concentration is expected to result in a larger percentage of Te (vs Se) surrounding a N atom, and thus lead to an activation energy closer to the ZnTe value.

We further would like to point out two important practical aspects, which arise from the above discussions. First, since the acceptors are now not located within ZnSe, but rather in a "favorable" ZnTe-rich environment, one can attempt to use other dopants (e.g., As, P, or Sb) which give high carrier concentrations in ZnTe, but have not succeeded in ZnSe. In addition, we again note, and this is quite important, that there is strong evidence that nitrogen itself could be a culprit in device degradation.[13,15] Second, a similar approach could be applied to achieving adequate *p*-type doping of other wide-band-gap semiconductors, including ZnO and $Al_xGa_{1-x}N$ with $x \geq 0.15$, materials currently of high physical and technological importance, for which, however, good *p*-type doping is still difficult to attain.[33] It appears that if one uses co-δ-doping with As, it would be equivalent to the above ZnSeTe system. In fact, GaAs can be *p*-type doped relatively easily using Mg, C, or Be (we note that the C site is equivalent to the N site in ZnSe); moreover, these are smaller than As, which in turn is larger than N, so the same driving forces for nanoisland formation are expected.

TABLE I. Sample parameters and PL properties.

Te concentration	$N_A - N_D$ (cm^{-3})	PL quenching activation energy (meV)
$<3.0\%$	$\sim 6.0 \times 10^{18}$	38
$\sim 1.3\%$	$\sim 4.0 \times 10^{18}$	72
$<1.0\%$	$\sim 3.0 \times 10^{18}$	87

In summary, we have shown the existence of N-doped ZnTe-rich nanoislands in δ^3-ZnSe:(Te,N) multilayers, grown by MBE, using N as a dopant and Te as a codopant to facilitate the incorporation of N. These nanoislands are certainly unusual, and may well be unique, providing vastly improved doping in at least one semiconductor system. The proof for these islands is provided by TEM, which showed a periodic structure of sub-monolayer islands; by HRXRD, which showed the islands to be Te-rich; by SIMS in conjunction with ECV profiling, which showed that both N and Te stay together within the δ^3-regions; and by the temperature quenching of PL, which showed that the resultant values of the N acceptor activation energies are consistent with N being embedded preferentially in a ZnTe-rich environment.

We acknowledge support from DOE under Grants No. DE-FG02-98ER45694 and No. DE-FG02-98ER45695, and Division of Materials Sciences, Office of Basic Energy Science DOE, Contract No. DE-AC02-98CH10886.

---

*Corresponding author. Email address: Igor_Kuskovsky@qc.edu

†Present address: Northwestern University.

[1] G. F. Neumark, Phys. Rev. Lett. **62**, 1800 (1989).

[2] G. F. Neumark, R. M. Park, and J. M. DePuydt, Phys. Today **47** (6), 26 (1994).

[3] G. F. Neumark, Mater. Lett. **30**, 131 (1997).

[4] G. F. Neumark, Mater. Sci. Eng., R. **21**, 1 (1997).

[5] C. G. Van de Walle, D. B. Laks, G. F. Neumark, and S. T. Pantelides, Phys. Rev. B **47**, 9425 (1993).

[6] D. B. Laks, C. G. Van de Walle, G. F. Neumark, and S. T. Pantelides, Appl. Phys. Lett. **63**, 1375 (1993).

[7] S. B. Zhang, S. H. Wei, and A. Zunger, Phys. Rev. Lett. **84**, 1232 (1999).

[8] D. J. Chadi, Phys. Rev. B **59**, 15181 (1999).

[9] W.-C. Lin, M. C. Tamargo, I. Kuskovsky, C. Tian, and G. F. Neumark, Appl. Phys. Lett. **76**, 2205 (2000).

[10] S. P. Guo, W.-C. Lin, X. Zhou, M. C. Tamargo, C. Tian, I. Kuskovsky, and G. F. Neumark, J. Appl. Phys. **90**, 1725 (2001).

[11] W. Lin, B. X. Yang, S. P. Guo, A. Elmouni, F. Fernandez, and M. C. Tamargo, Appl. Phys. Lett. **75**, 2608 (1999).

[12] Single δ-doped samples will have fewer ZnTe-rich nanoislands capable of providing good *p*-type doping. These single-δ layers also improved *p*-type doping (compare with the bulk) but by factor of 4–6 lower than triple-δ layers.

[13] V. N. Jmerik, S. V. Sorokin, T. V. Shubina, N. M. Shmidt, I. V. Sedova, D. L. Fedorov, S. V. Ivanov, and P. S. Kop'ev, J. Cryst. Growth **214/215**, 502 (2000).

[14] Igor L. Kuskovsky, G. F. Neumark, J. G. Tischler, and B. A. Weinstein, Phys. Rev. B **63**, 161201(R) (2001).

[15] N. Yu. Gordeev, S. V. Ivanov, I. I. Novikov, T. V. Shubina, N. D. Ilinskaya, S. P. Kopev, G. Reuscher, A. Waag, and G. Landehr, Phys. Status Solidi B **229**, 1019 (2002).

[16] S. Gundel and W. Faschinger, Phys. Rev. B **65**, 035208 (2002).

[17] We note that most of the other systems have different metals, which are simpler to resolve in TEM. In our case the contrast between Te and Se, especially in the case of low Te concentration, is very difficult to detect.

[18] Taking the Gaussian as $I(q)=(1/\sigma\sqrt{2\pi})\exp(-q^2/2\sigma^2)$ one obtains that 95% of all q values will be within the 4σ interval.

[19] Y. Gu, Igor L. Kuskovsky, M. van der Voort, G. F. Neumark, X. Zhou, M. Muñoz, and M. C. Tamargo, Phys. Status Solidi B **241**, 515 (2004).

[20] H. F. Yan, Ph.D. dissertation, Columbia University, 2005.

[21] D. Keith Bowen and Brian K. Tanner, *High Resolution X-ray Diffractometry and Topography* (Taylor & Francis, London, 1998), Chap. 6.

[22] Y. Gu, Igor L. Kuskovsky, M. van der Voort, G. F. Neumark, X. Zhou, and M. C. Tamargo, Phys. Rev. B **71**, 045340 (2005).

[23] We note that the knowledge of hole concentration is essential for confirming the improved p-type doping. However, in practice, the Hall effect is difficult to measure, even in Van der Pauw geometry, in the absence of reliable Ohmic contacts [see e.g., P. M. Mensz *et al.*, Appl. Phys. Lett. **63**, 2800 (1993); NIST, http://www.eeel.nist.gov/812/effe.htm#evol; David C. Look, *Electrical Characterization of GaAs Materials and Devices* (Wiley, New York, 1989), Chap. 1], which are hard to fabricate in p-type ZnSe because of the surface Fermi level pinning [e.g., Y. Koide *et al.*, J. Appl. Phys. **82**, 2393 (1997)]. Moreover, it is even less accurate for materials with low free-carrier mobility [D. Marioli and V. Varoli, J. Phys. E **16**, 892 (1983)], which is the case of p-type ZnSe.

[24] C. G. Van de Walle, D. B. Laks, G. F. Neumark, and S. T. Pantelides, Phys. Rev. B **47**, 9425 (1993).

[25] This sample was design with SIMS measurements in mind, since the resolution of the technique is somewhat limited; also, additional information about the Te concentrations as functions of deposition time has been obtained.

[26] SIMS resolution decreases with increasing depth.

[27] Igor L. Kuskovsky, C. Tian, C. Sudbrack, G. F. Neumark, W.-C. Lin, S. P. Guo, and M. C. Tamargo, J. Appl. Phys. **90**, 2269 (2001).

[28] These values were obtained from the high-temperature slope of the peak intensity vs T^{-1}; we also used a temperature prefactor of $T^{3/2}$ in the fitting formula, where this arises from the density of states, with comparable results.

[29] P. J. Dean, W. Stutius, G. F. Neumark, B. J. Fitzpatrick, and R. N. Bhargava, Phys. Rev. B **27**, 2419 (1983).

[30] N. J. Duddles, K. A. Dhese, P. Devine, D. E. Ashenford, C. G. Scott, J. E. Nicholls, and J. E. Lunn, J. Appl. Phys. **76**, 5214 (1994).

[31] Y. Fan, J. Han, L. He, J. Saraie, R. L. Gunshor, M. Hagerott, and A. V. Nurmikko, J. Electron. Mater. **23**, 245 (1994).

[32] H. D. Jung, C. D. Song, S. Q. Wang, K. Arai, Y. H. Wu, Z. Zhu, T. Yao, and H. Katayama-Yoshida, Appl. Phys. Lett. **70**, 1143 (1997).

[33] See, e.g., http://www.darpa.mil/mto/suvos/index.html